Available at www.sciencedirect.com

SciVerse ScienceDirect

journal homepage: www.elsevier.com/locate/carbon

Highly dispersed carbon nanotubes in organic media for polymer:fullerene photovoltaic devices

Gwang H. Jun, Sung H. Jin, Sung H. Park, Seokwoo Jeon, Soon H. Hong *

Department of Material Science and Engineering, Korea Advanced Institute of Science and Technology (KAIST), 335 Science Rd., Daejeon 305-701, Republic of Korea

ARTICLE INFO

Article history:
Received 10 June 2011
Accepted 29 July 2011
Available online 12 August 2011

ABSTRACT

Composites for a photo-active layer in an organic photovoltaic device are fabricated using homogeneously dispersed carbon nanotubes (CNTs) in a polymer:fullerene bulk-heterojunction matrix. CNTs are functionalized by alkyl-amide groups for high dispersion in organic media and by homogeneously mixing them with the polymer and fullerene in solution. In a Fourier transform infrared spectrometry analysis, the formation of functional groups is confirmed. Scanning electron microscopy images indicate the high dispersion of the CNTs. These composites show considerable improvement of their optical and electrical properties due to effects of the wideband photo-absorption and high charge carrier mobility of the CNTs. These effects were investigated by ultraviolet–visible spectroscopy and by the fabrication of an organic thin film transistor. An organic solar cell was fabricated from these composites as a photo-active layer, showing a remarkable 40% (3.2–4.4%) increase of the power conversion efficiency compared to an organic solar cell using a photo-active layer without CNTs.

1. Introduction

Organic photovoltaic (OPV) materials promise the production of low-cost and large-area devices on flexible substrates [1,2]. However, the main drawback is the low power conversion efficiency (PCE). The main reason for the low PCE is the extremely short exciton diffusion length (~10 nm) in organic materials as compared to highly ordered inorganic materials [3]. Excitons generated only within the short distance between donor–accepter interfaces dissociate into free electrons and holes that contribute to photovoltaic generation without exciton decay. Recently, bulk-heterojunction (BHJ) structures were employed to multiply the number of dissociation sites by increasing the interface area [4,5]. The increased area increases the opportunity for excitons to dissociate into charge carriers, which results in better PCE. However, the transport length of the charge carriers toward each electrode is limited by the low electron and hole mobilities ($<10^{-4}$ cm^2 V^{-1} s) of the organic materials [5].

The introduction of one-dimensional (1D) nanostructures such as carbon nanotubes (CNTs) not only provides charge carriers with highly conductive pathways with high carrier mobility, but also offers a broad absorption band that is expanded into the near-infrared range due to the small energy band gap of the CNTs [6–8]. Furthermore, due to the spatial separation of the charges across the donor–acceptor interface, photoexcitation of the polymer easily gives rise to carriers with other carbon materials such as CNT, graphene and fullerene [9–11]. Despite these advantages, OPV with CNTs incorporated in their photoactive layers have demonstrated significantly poorer efficiency than those without CNTs [12,13]. The key step to improve the performance of OPV through CNT mixing is the uniform blending of CNTs and photoactive polymers or fullerenes [14]. Chaudhary et al. reported a device with CNTs

* *Corresponding author:* Fax: +82 42 350 3310.
E-mail address: shhong@kaist.ac.kr (S.H. Hong).
0008-6223/$ - see front matter
doi:10.1016/j.carbon.2011.07.052

embedded in the photoactive layer [15]. However, it shows low performance due to a reduction in its JSC value because the non-homogeneously dispersed CNTs cause a disruption of the optimized morphology of the active layer (e.g., nanoscale phase separation of the donor and the acceptor) [4,5]. Moreover, the agglomerated CNTs act as recombination sites for charge carriers [16].

In this work, we propose a new means of dispersing CNT homogeneously in a polymer:fullerene bulk-heterojunction matrix (CNT/polymer:fullerene composites). Functionalization of CNTs with an alkyl-amide group enhances the hydrophobicity and steric hindrance between the CNTs. Through these effects, the functionalized CNTs become well dispersed in organic solvents and can be mixed homogeneously with semiconducting polymer, poly 3-hexylthiophene (P3HT) and a fullerene derivative, [6,6]-phenyl C61 butyric acid methyl ester (PCBM) in a solution without a sonication process.

The removal of sonication is important to minimize the breakage of the polymer chains and the degradation of the optoelectronic properties. The effect of this functionalization on the dispersibility is characterized by Fourier transform infrared spectroscopy (FT-IR) and scanning electron microscopy (SEM). The FT-IR and SEM results reveal that our method improves the dispersibility of CNTs and the morphology of the active layer. CNT/polymer:fullerene composites showed a large improvement of their optical and electrical properties, including their charge carrier mobility (μ, from -2.01×10^{-4} to -4.64×10^{-4} cm^2/Vs). The fabrication and characterization of the OPV material with functionalized CNTs in the active layer show that the device performance improved by 30% (3.2–4.4%) in terms of the PCE as compared to an organic solar cell without CNTs due to the effects of the wideband photo-absorption and high charge carrier mobility, as mentioned above. These effects are investigated by ultraviolet–visible (UV–Vis) spectroscopy and by the fabrication of an organic thin film transistor (OTFT).

2. Experimental section

2.1. Functionalization of carbon nanotubes

HiPco single wall carbon nanotubes (SWCNTs) supplied by Unidym, Inc. with diameters of 0.8–1.2 nm were purified by oxidation and HCl treatment. The CNTs were oxidized in air at 225 °C for 18 h to remove the amorphous carbon and were then sonicated for 1 h in conc. HCl to extract any metal impurities from the SWNTs. Five milligram of purified SWNTs were sonicated for 1 h with a mixed solution of HNO_3/H_2SO_4 at a ratio of 1:3 for carboxylate functionalization. After the functionalization of the SWNTs via the carboxylate group (carboxylate CNT), 100 mg of SWNTs were stirred in 20 ml of $SOCl_2$ containing 1 ml of dimethylformamide (DMF) at 70 °C for 24 h. After centrifugation, the brown-colored supernatant was decanted and the remaining solid was washed with anhydrous tetrahydrofuran (THF). After centrifugation, the pale yellow supernatant was decanted. The remaining solid was dried at room temperature under a vacuum. A mixture of the resulting CNTs and 2 g of ODA (melting point, 55–57 °C) was heated at 90–100 °C for 96 h. After cooling to room temperature, the excess ODA was removed by washing with ethanol four times (5–10 min of sonication at 40 KHz). The remaining solid was dissolved in dichloromethane, and after filtration, the black filtrate was dried on a rotary evaporator. The resulting black solid was dried at room temperature under a vacuum.

2.1.1. Fabrication of CNT/P3HT:PCBM composites

These CNTs functionalized alkyl-amide group (alkyl-amide CNT) were diluted 1 mg for 10 ml in chlorobenzene by 1hr of sonication. The P3HT, supplied by Rieke Metals, and PCBM supplied by Sigma Aldrich were dissolved and stirred in 1 ml if chlorobenzene for 12 h each. Alkyl-amide CNT versus P3HT of 0, 0.1, 0.2, and 0.3 wt.% were mixed in solution states. With the CNTs, 0.3 wt.% of P3HT in chlorobenzene is the maximum concentration that could be obtained to achieve a homogeneous solution. An increase of this concentration generally led to precipitation of the CNTs.

2.2. Fabrication of OPV using CNT/P3HT:PCBM composites

Indium Tin Oxide (ITO)-coated glass, supplied by Samsung Corning Co., Ltd., was cleaned with 2-propanol and a mixture of NH_3 and H_2O_2. An O_2 plasma treatment was then conducted to improve the wetting between the ITO and the poly(3,4-ethylenedioxythiophene):poly(styrenesulfonate) (PEDOT:PSS) (solid content: 2.2–2.6 wt.% in H_2O), which was purchased from Sigma Aldrich. The solutions were spin coated on ITO at 1000 rpm for 1 min and then baked at 120 °C for 10 min. The P3HT and PCBM were dissolved and stirred in 1 ml of chlorobenzene for 12 h each. The alkyl-amide CNTs were mixed with a blend of P3HT and PCBM which was made by the mixing of two solutions for 12 h (ratio of P3HT:PCBM = 1:0.8). The blend of CNTs, P3HT and PCBM was spin-coated on the PEDOT:PSS at 300 rpm for 1 min in a glove box filled with N_2 gas. An Al electrode was thermally evaporated in a vacuum at a pressure of 10^{-7} torr. Finally, the device was directly placed on a digital hot plate at 150° for 5 min.

2.3. Characterizations of the functionalized CNT, CNT/P3HT:PCBM composites and OPV using CNT/P3HT:PCBM composites

Microstructural observation of the functionalized CNTs and CNT/P3HT:PCBM was carried out via scanning electron microscopy (Hitachi S-480). Before the observation of the microstructure, an Ar plasma treatment of CNT/P3HT:PCBM was conducted using a plasma cleaner (Aaron Ribner Plasmatic Systems, Inc.). The FT-IR and UV–Vis spectroscopy used in this work were done using a FT-IR spectrometer from Jasco (FT/IR-4100) and a UV–Vis spectrometer from Simadzu (UV-3101 PC). The organic thin-film transistors (OTFTs) were fabricated using the bottom gate configuration on highly doped n-type Silicon (Si) substrates with a gate electrode with thermally grown silicon oxide of 300 nm (SiO_2) as a dielectric layer. The substrate was cleaned carefully and hexamethyldisilazane (HMDS) was spin-coated at 7500 rpm for 35 s under a N_2 atmosphere inside a glove box. Alkyl-amide CNTs at various concentrations (0.1, 0.2, 0.3 wt.% with respect to P3HT) were sonicated for 30 min

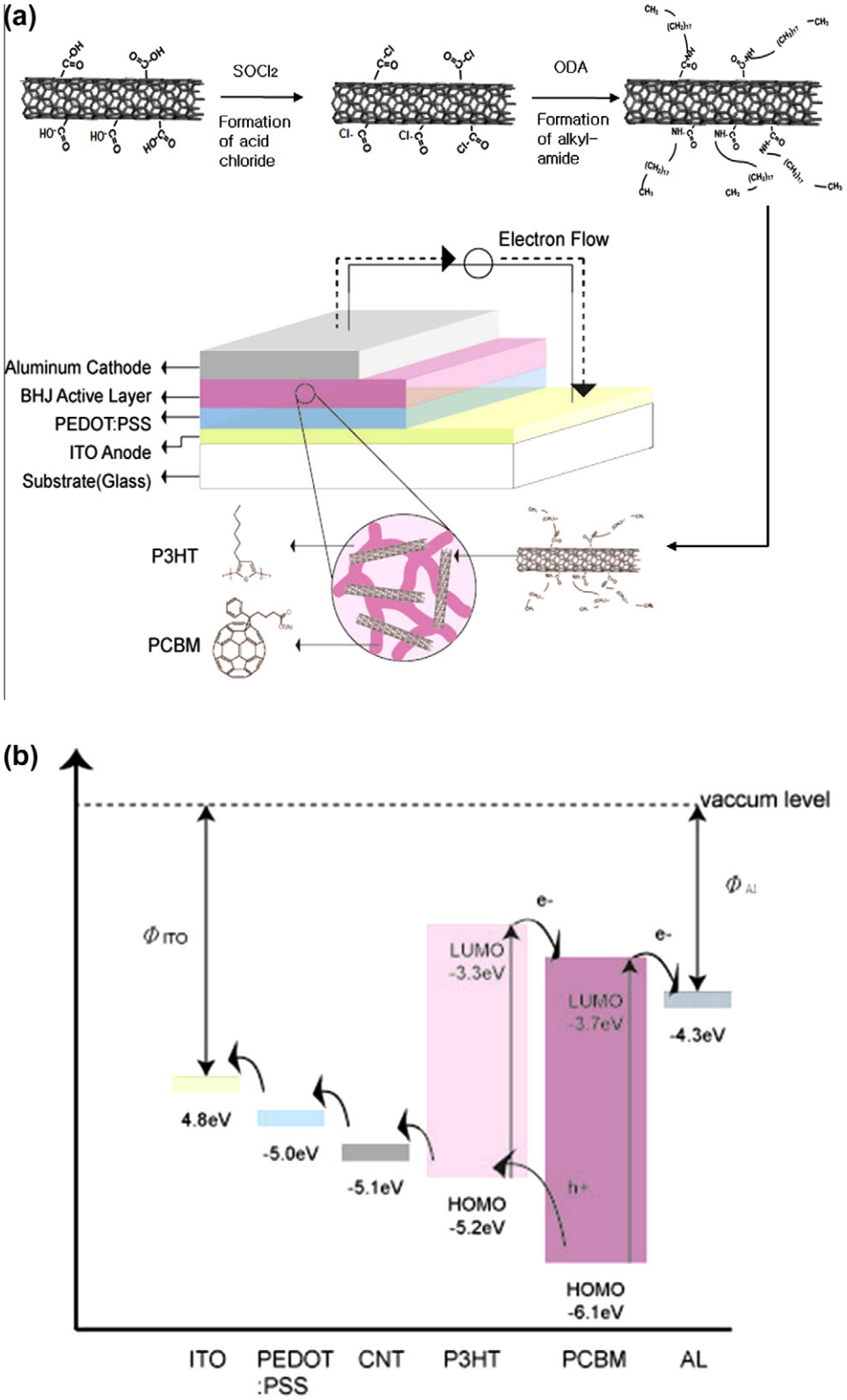

Fig. 1 – Schematics of the functionalization of CNTs by the alkyl-amide functional group for a homogeneous dispersion in organic solvent and the devices fabricated in this work: (a) energy-level diagram of a CNT/P3HT:PCBM BHJ solar cell showing the charge generation and transfer between the two organic components to the electrodes (b).

and added to the P3HT:PCBM solution in chloroform. The solution was spin-coated at 2000 rpm fir 60 s from a 0.5 wt.% chloroform solution with an average thickness 50 nm under a N_2 atmosphere inside a glove box. A gold (Au) layer (thickness:

50 nm) was thermally evaporated onto the top of the semiconductor through a designed shadow mask in a vacuum chamber for the source and drain electrodes (channel width, $W = 1500\ \mu m$, channel length, $L = 100\ \mu m$).

The photovoltaic properties of the OPV were characterized under 1-sun strength using a xenon lamp with an AM 1.5 global filter. A silicon reference solar cell certified by the National Renewable Energy Laboratory (NREL) was used to calibrate the light and confirm the measurement conditions. Current–voltage (*I–V*) measurements were performed using an electrochemical analyzer by Ivium CompactStat. In both OPV and OTFT characterizations, the entire test is repeated for the four devices for each set of fabrication conditions.

3. Results and discussion

Fig. 1 shows a schematic illustration of a conventional P3HT:PCBM bulk-heterojunction cell with functionalized CNTs (Fig. 1a) and an energy level diagram (Fig. 1b) along with the general procedure of incorporating the CNTs into an active layer. The use of single-wall carbon nanotubes (SWCNTs) promotes charge-selectively properties due to the semiconducting band gap structures, as indicated in Fig. 1b [17].

CNTs have intense cohesiveness due to the strong van der Waals force between the CNTs caused by their large mass-to-surface ratio originating from their nanoscale size and high aspect ratio [18,19]. Thus, the surface functionalization of CNTs is an important step in the introduction of CNTs into polymer:fullerene BHJ composites. The functionalization of CNTs is identified by FT-IR analysis, as shown in Fig. 2c. The FT-IR spectrum of pristine CNTs does not show any peaks corresponding to functional groups on the surface of the CNTs. However, after functionalization, peaks at $\upsilon = 1680–1720\ cm^{-1}$ (C=O stretch) appear in the FT-IR results (Fig. 2c). These peaks come from carboxylate groups that are covalently functionalized on the CNTs (carboxylate CNT) by a substitution process that occurs during the acid treatment [20].

Due to the attached carboxylate groups (–COOH), the electrostatic repulsive force between the CNTs overcomes the van der Waals' force to form a stable suspension within the solvent. For this reason, carboxylate CNT indicates an excellent incohesive property in a hydrophilic solution but not in a hydrophobic solution [21,22]. To improve the high incohesive property in a hydrophobic solution such as chlorobenzene, we functionalized CNTs with an alkyl-amide group (alkyl-amide CNT) via a condensation process between carboxylate and amide groups. The solid obstacle effect of the alkyl-amide group on the CNTs makes them disperse uniformly in an organic solvent. FT-IR peaks at 2845 and 2917 cm^{-1} relevant to the C–H stretch by the alkyl chain in the CNTs prove the successful functionalization of alkyl-amide CNTs.

The stable homogeneous dispersion of alkyl-amide CNTs remained intact without any precipitation after 3 weeks (Fig. 2b inset), whereas the carboxylate CNT did not (Fig. 2a inset). SEM images of spin-coated carboxylate and alkyl-amide CNT dissolved in chloroform, followed by drying on a Si wafer, are shown in Fig. 2a and b, respectively. The carboxylate CNTs remain highly bundled and agglomerated as in the solvent, while the alkyl-amide CNTs exhibit a highly homogeneous dispersion. These results demonstrate that the functionalization of CNTs by an alkyl-amide group is an effective method to dis-

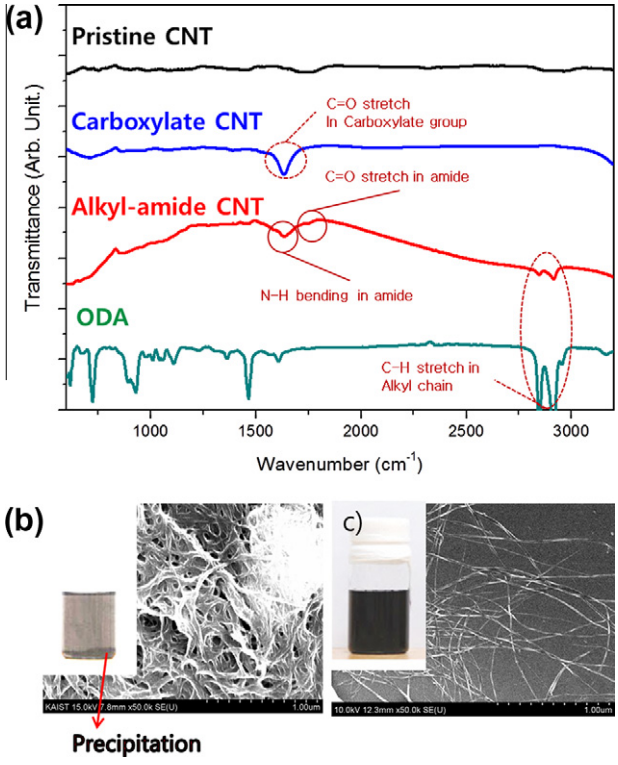

Fig. 2 – Photograph and SEM images of functionalized CNTs by carboxylate (a) and alkyl-amide (b) dispersion in chlorobenzene after 3 days, (c) FT-IR results of the functionalized CNTs (scale bar is 1 μm).

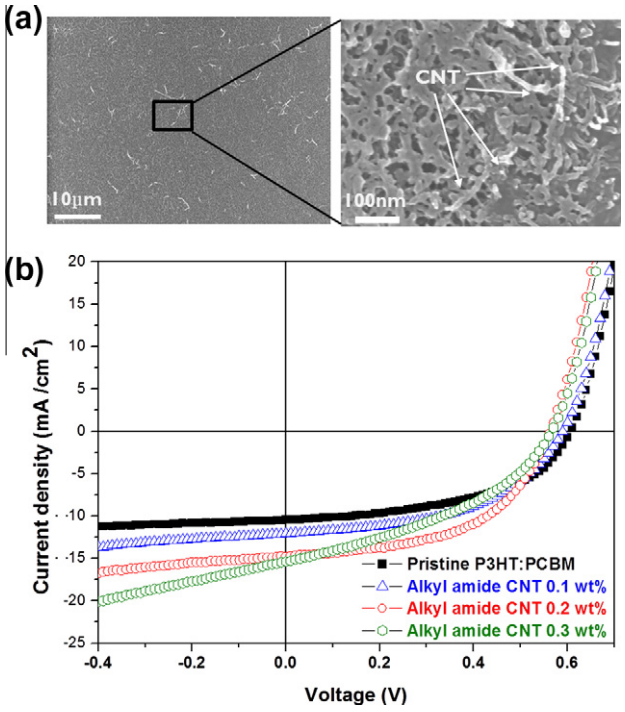

Fig. 3 – SEM image of alkyl-amide CNT/P3HT:PCBM composites and a high-magnification image after Ar-plasma etching (a). *I–V* curves of OPV using alkyl-amide.

perse CNTs in a hydrophobic media. The alkyl-amide CNT could be mixed homogeneously with a polymer:fullerene in a solution state.

The homogenous dispersion of CNTs is accomplished throughout the thickness of spin-coated CNT/P3HT:PCBM composite film. The properties of the organic solar cell fabricated from these homogeneously dispersed CNT composites as a photoactive layer shows 40% increase of the power conversion efficiency (PCE) compared to an organic solar cell without CNT (3.2–4.4%). The SEM images in Fig. 3a show the inner microstructures of the composite film, where the alkyl-amide CNT is incorporated into the polymer:fullerene matrix.

The film underwent an Ar plasma treatment of 1 min to expose the inner layer of the composite film. Fig. 3b shows a plot of the I–V characteristics under AM 1.5 simulated solar radiation as a reference using a P3HT:PCBM solar cell and with a CNT/P3HT:PCBM composite solar cell. The photovoltaic parameters are given in Table 1. It is clear that the solar cell using the CNT/P3HT:PCBM composites increases the PCE more, from 3.2% to 4.4%, compared to the reference solar cell using P3HT:PCBM (without CNT) as the CNT concentration increased. The open circuit voltage (V_{OC}) decreases slightly due to the small energy level variation of the active layer when CNTs were used in the P3HT:PCBM. The results show that the PCE increase mainly originates from the increase of the short circuit current (J_{SC}, from 10.5 to 14.6 mA/cm^2). The increase in the photocurrent caused by the incorporated CNTs was likely due to two major factors. The first is the increase of the absorbed photons, and the second is increase of the charge carrier mobility.

Fig. 4a shows the normalized UV–Vis absorption spectroscopy of the diluted solutions of alkyl-amide CNT/P3HT:PCBM composites in chlorobenzene. The concentration of the CNT is very low in the solution (0–0.2 wt.%). Therefore, the characteristics of the Van Hove singularity absorption waves of the SWCNTs are not observable. Due to the band gap structure of the SWNT (~0.8 ev), CNT can absorb photons with a wavelength in the infrared region [6]. There is considerably high absorption in the infrared region between 800 and 1600 nm according to the UV–Vis absorption spectroscopy results. This can lead to incident light scattering by the enlarged surface area and photocurrent as the surface roughness increases with the incorporated CNTs (see Supporting Information, Fig. S1) [23].

To investigate the effect of the increase in the charge carrier mobility caused by the incorporated CNT, we fabricated and characterized an organic thin film transistor (OTFT). Fig. 4c shows the output characteristics of the reference using P3HT:PCBM device and the CNT/P3HT:PCBM composite devices used here. The characteristics of the devices exhibit the typical drain voltage (V_d) and drain current (I_d) characteristics of OTFTs as they operate in accumulation mode with a negative gate bias, V_g. The output current of the CNT/P3HT:PCBM composites device used here is higher than that of the reference P3HT:PCBM device as the CNT concentration increases. The field-effect mobility is calculated from the slope in the transfer saturation region (Fig. 4b) when the drain current (I_{DS}) is plotted against the gate voltage (V_{GS}) [24]. The data is fitted to the following equation:

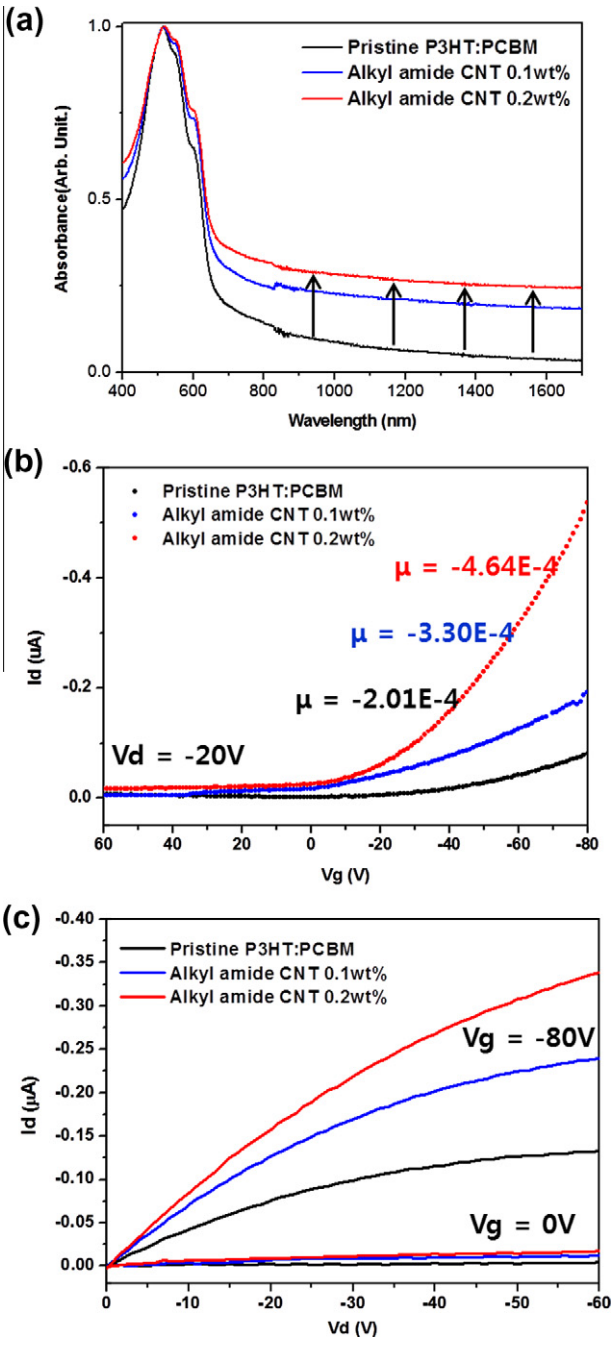

Fig. 4 – (a) Normalized UV–Vis absorption spectra, (b) Transfer characteristics, (c) output characteristics of OTFT devices of the alkyl-amide CNT/P3HT:PCBM composites solution (red and blue line) and a reference solution of only P3HT:PCBM (black line) in chlorobenzene. (For interpretation of the references to colour in this figure legend, the reader is referred to the web version of this article.)

$$I_{ds} = \frac{W}{2L} C_i \mu (V_G - V_T)^2 \quad (1)$$

Here, I_{DS} is the drain current, μ is the carrier mobility, V_T is the threshold voltage, C_i is the gate oxide capacitance ($C_i = 10.8 \times 10^{-9}$ F cm^2), W is the channel width (W = 1500 μm), and L is the channel length (L = 100 μm). The calculated field-ef-

Table 1 – Photovoltaic parameters of OPV in this work.

	J_{SC} (mA/cm^2)	V_{OC} (V)	FF	PCE (%)
Pristine P3HT:PCBM	10.45 ± 0.657	0.6 ± 0.005	0.50 ± 0.014	3.18 ± 0.152
Alkyl-amide CNT 0.1 wt.%	12.08 ± 0.221	0.59 ± 0.003	0.50 ± 0.009	3.54 ± 0.130
Alkyl-amide CNT 0.2 wt.%	14.79 ± 1.114	0.56 ± 0.012	0.52 ± 0.016	4.39 ± 0.294
Alkyl-amide CNT 0.3 wt.%	15.39 ± 0.490	0.56 ± 0.031	0.38 ± 0.024	3.38 ± 0.421

fect mobility of pure P3HT:PCBM is -2.01×10^{-4} cm^2/Vs. With the 0.2 wt.% CNT-incorporated P3HT:PCBM, the field-effect mobility is -4.64×10^{-4} cm^2/Vs, which is twice as high as pure P3HT:PCBM, revealing that the CNT/P3HT:PCBM composites show higher field-effect mobility than P3HT:PCBM. This improvement of the field-effect mobility could result from the fact that the CNTs act as an effectively charge carrier pathway due to the homogeneous dispersion.

4. Conclusion

In summary, we report alkyl-amide CNTs which can be homogeneously mixed with photoactive materials such as P3HT and PCBM in a solution because both the alkyl-amide CNTs, P3HT and PCBM have high dispersibility in organic solvents. When CNTs are homogeneously mixed in the photoactive layer of an organic solar cell, the CNTs can absorb light at the infrared wavelength, which increases the optical absorption of organic solar cells. Crucially, according to an analysis of the device property by the fabrication and characterization of an OTFT, the charge carrier mobility nearly doubled due to the introduction of CNTs. Several researchers have reported that the chemical functionalization of CNTs creates many defects on their surfaces and thus degrades their electronic properties [25]. However, even if an acid treatment affected CNT surfaces and caused defects, a compromise can been found with the increase of the mobility and the short circuit current density, as CNTs have extremely high electrical properties compared to polymer:fullerene BHJ matrix.

The high electrical conductivity leads to an increase in the photocurrent, which can improve the overall efficiency of the device. The efficiency was significantly increased from 3.2% to 4.4% when the solar cells were manufactured with alkyl-amide CNTs, which can be dispersed homogeneously in a hydrophobic organic solvent.

Acknowledgements

This research was supported by Future-based Technology Development Program (Nano Fields) through the National Research Foundation of Korea (NRF) funded by the Ministry of Education, Science and Technology (Grant No. 2010-0019132). It was also partially supported by Basic Science Research Program through the National Research Foundation of Korea (NRF) funded by the Ministry of Education, Science and Technology (MEST: 2009-0066879).

Appendix A. Supplementary data

Supplementary data associated with this article can be found, in the online version, at doi:10.1016/j.carbon.2011.07.052.

REFERENCES

[1] Yu G, Gao J, Hummelen JC, Wudl F, Heeger AJ. Polymer photovoltaic cells: enhanced efficiencies via a network of internal donor–acceptor heterojunctions. Science 1995;270:1789–91.
[2] Sariciftci NS, Smilowitz L, Heeger AJ, Wudl F. Photoinduced electron transfer from a conducting polymer to buckminsterfullerene. Science 1992;258:1474–6.
[3] Kannan B, Castelino K, Majumdar A. Design of nanostructured heterojunction polymer photovoltaic devices. Nano Lett 2003;3:1729–33.
[4] Ma WL, Yang CY, Gong X, Lee KH, Heeger AJ. Thermally stable, efficient polymer solar cells with nanoscale control of the interpenetrating network morphology. Adv Funct Mater 2005;15:1617–22.
[5] Li G, Shrotriya V, Huang JS, Yao Y, Moriarty T, Emery K, et al. High-efficiency solution processable polymer photovoltaic cells by self-organization of polymer blends. Nat Mater 2005;4:864–8.
[6] Berson S, Bettignies RD, Bailly S, Guillerez S, Jousselme B. Elaboration of P3HT/CNT/PCBM composites for organic photovoltaic cells. Adv Funct Mater 2007;17:3363–70.
[7] Wei J, Jia Y, Shu Q, Gu Z, Wang K, et al. Double-walled carbon nanotube solar cells. Nano Lett 2007;7:2317–21.
[8] Li X, Jia Yi, Wei J, Zhu H, Wang K, et al. Solar Cells and light sensors based on nanoparticle-grafted carbon nanotube films. ACS Nano 2010;4(4):2142–8.
[9] Ferguson AJ, Blackburn JL, Holt JM, Kopidakis N, Tenent RC, et al. Photoinduced energy and charge transfer in P3HT:SWNT composites. J Phys Chem Lett 2010;1:2406–11.
[10] Yu D, Park K, Durstock M, Dai L. Fullerene-grafted graphene for efficient bulk heterojunction polymer photovoltaic devices. J Phys Chem Lett 2011;2:1113–8.
[11] Pensack RD, Asbury JB. Beyond the adiabatic limit: charge photogeneration in organic photovoltaic materials. J Phys Chem Lett 2010;1:2255–63.
[12] Liu J, Tanaka T, Sivula K, Alivisatos AP, Fréchet JMJ. Employing end-functional polythiophene to control the morphology of nanocrystal–polymer composites in hybrid solar cells. J Am Chem Soc 2004;126(21):6550–1.
[13] Arranz-Andrés J, Blau WJ. Enhanced device performance using different carbon nanotube types in polymer photovoltaic devices. Carbon 2008;46:2067–75.
[14] Miller AJ, Hatton RA, Silva SRP. Interpenetrating multiwall carbon nanotube electrodes for organic solar cells. Appl Phys Lett 2006;89(1–3):133117-1–3.
[15] Chaudhary S, Lu HW, Meuller AM, Bardeen CJ, Ozkan M. Hierarchical placement and associated optoelectronic impact of carbon nanotubes in polymer-fullerene solar cells. Nano Lett 2007;7:1973–9.
[16] Ago H, Petritsch K, Shaffer MSP, Windle AH, Friend RH. Composites of carbon nanotubes and conjugated polymers for photovoltaic devices. Adv Mater 1999;11:1281–5.
[17] Liu L, Li G. Electrical characterization of single-walled carbon nanotubes in organic solar cells by Kelvin probe force microscopy. Appl Phys Lett 2010;96(1–3):083302-1–3.

[18] Thess A, Lee R, Nikolaev P, Dai H, Petit P, Robert J, et al. Crystalline ropes of metallic carbon nanotubes. Science 1996;273:483–7.
[19] Ajayan PM, Tour JM. Nanotube composites. Nature 2007;447:1066–8.
[20] Cha SI, Kim KT, Arshad SN, Mo CB, Hong SH. Extraordinary strengthening effect of carbon nanotubes in metal-matrix nanocomposites processed by molecular-level mixing. Adv Mater 2005;17:1377–81.
[21] Kuznetsova A, Mawhinney DB, Naumenko V, Yates Jr JT, Liu J, Smalley RE. Enhancement of adsorption inside of single-walled nanotubes: opening the entry ports. Chem Phys Lett 2000;321:292–6.
[22] Ebbsen TW, Hiura H, Bischer ME. Decoration of carbon nanotubes. Adv Mater 1996;8:155–7.
[23] Lee JH, Kim DW, Jang H, Choi JK, Geng J, Jung JW, et al. Enhanced solar-cell efficiency in bulk-heterojunction polymer systems obtained by nanoimprinting with commercially available AAO membrane filters. Small 2009;5:2139–43.
[24] Sze SM. Physics of semiconductor devices. second ed. New York: Wiley; 1981. 440–451.
[25] Zhang X, Sreekumar TV, Liu T, Kumar S. Properties and structure of nitric acid oxidized single wall carbon nanotube films. J Phys Chem B 2004;108:16435–40.